Materials and Design 68 (2015) 158–166

Contents lists available at ScienceDirect

Materials and Design

journal homepage: www.elsevier.com/locate/matdes

Investigations on the structure – Property relationships of electron beam welded Inconel 625 and UNS 32205

K. Devendranath Ramkumar *, R. Sridhar, Saurabh Periwal, Smitkumar Oza, Vimal Saxena, Preyas Hidad, N. Arivazhagan

School of Mechanical & Building Sciences, VIT University, Vellore 632014, India

ARTICLE INFO

Article history:
Received 19 October 2014
Accepted 20 December 2014
Available online 27 December 2014

Keywords:
Super alloy
Duplex stainless steel
Electron beam welding
Mechanical properties
Microstructure

ABSTRACT

The metallurgical and mechanical properties of electron beam welded Ni based superalloy Inconel 625 and UNS S32205 duplex stainless steel plates have been investigated in the present study. Interface microstructure studies divulged the absence of any grain coarsening effects or the formation of any secondary phases at the heat affected zone (HAZ) of the electron beam (EB) weldments. Tensile studies showed that the fracture occurred at the weld zone in all the trials and the average weld strength was reported to be 850 MPa. Segregation of Mo rich phases was witnessed at the inter-dendritic arms of the fusion zone. The study recommended the use of EB welding for joining these dissimilar metals by providing detailed structure – property relationships.

1. Introduction

Dissimilar welds of nickel based superalloys and duplex stainless steel grades have significant advantages in geothermal and marine applications owing to their excellent mechanical properties and resistance to corrosion. Cal Energy, an independent power producer of electricity through geothermal power plant employed the pipes of Inconel 625 and Duplex stainless steel. It was vivid that the pipes of Inconel 625 were employed in high temperature and duplex stainless steels were operated in low temperature environments [1].

Richard [2] reported the typical use of bimetallic combinations of Inconel 625 and duplex stainless steel in the piping systems for sub-sea manifolds. The authors reported that use of less expensive material i.e. duplex stainless steel which brought down the cost without compromising the efficiency. Vandervoort [3] investigated the bimetallic joints of Inconel 625 and austenitic stainless steel obtained from Gas Tungsten Arc Welding (GTAW), Gas Metal Arc Welding (GMAW) and Shielded Metal Arc Welding (SMAW) processes. The authors reported that all the weldments offered better strength and toughness at low temperatures (4 K).

Sridhar et al. [4] investigated these bimetallic joints obtained from continuous current gas tungsten arc welding (CCGTAW) process employing two different filler metals such as ER2209 and ERNiCrMo-3. The authors reported that the use of ERNiCrMo-3 filler resulted in the formation of detrimental laves phases which severely deteriorated the mechanical properties. Further the authors added that the multi-pass welding resulted in the reheating zones and the slow cooling rates were the factors that resulted in adverse metallurgical and mechanical properties.

As claimed by researchers [5,6], the welding of two metals involving different compositions and coefficients of thermal expansion is cumbersome as the resultant weldments have greater susceptibility to heat affected zone (HAZ) liquation cracking, solidification cracking and residual stresses. The probability of obtaining these metallurgical problems is greater for the conventional welding processes such as GTAW, GMAW and SMAW. Moreover the selection of filler metal is also crucial issue in employing these techniques. Mismatching in composition of the base and filler metal tends to lower the yield strength due to the agglomeration of large amount of residual stresses during the joining process.

Electron Beam Welding (EBW) is one of the widely used joining techniques for thicker sections and enjoys several advantages including the absence of secondary phases, higher depth to width ratio, reduced residual stress and distortion and the possibility of automation. Kuo [5] reported that due to higher cooling rates, finer grains with good weld mechanical properties could be established while employing EB welding compared to arc welding processes. Devendranath Ramkumar et al. [6] carried out the investigations on the electron beam welded super-duplex stainless steel UNS S32750. The authors reported the absence of grain coarsening effects at the region adjacent to the fusion zone owing to the faster

* Corresponding author. Tel.: +91 416 220 2184.
E-mail address: deva@vit.ac.in (K. Devendranath Ramkumar).

http://dx.doi.org/10.1016/j.matdes.2014.12.032
0261-3069/

cooling rates. The formation of coarser ferrite morphology with the presence of inter and intra-granular austenite and the absence of Widmänstatten side plates of austenite during EBW was reported by the authors. Sun and Karppi [7] reported that EB welding reduces or overcomes the problems such as uneven heat dissipation, formation of brittle phases to certain extent, and hence produces satisfactory joints compared to other joining techniques. The authors addressed that as EB welding employed low total-heat input per unit length of weld, this technique can also reduce the residual stresses substantially, as compared to arc welding. Patterson and Milewski [8] observed the cracking at the fusion zone of dissimilar joints of Inconel 625 and AISI 304L while employing both autogenous GTA and PCGTA welding process. The authors claimed that the cracking susceptibility was due to the segregation of elements S, P and Nb to the interdendritic phase.

Madhusudan Reddy and Srinivasa Rao [9] investigated the similar and dissimilar welds of AISI 430, AISI 304 and AISI 2205 by friction and EB welding processes. The authors reported that the weldments obtained from EB welding process acquainted for better notch tensile strength. Further they reported the presence of residual stresses at the fusion region due to the delta ferrite. Venkata Ramana et al. [10] investigated the residual stress distribution of EB welds of Maraging steel and medium carbon steel. The authors reported that in the bimetallic welded joints, the magnitude of stresses could be lowered in the softer parent metal due to its stress absorbing nature. Shakil et al. [11] investigated the dissimilar welds of Inconel 625 and AISI 304L by EBW process. The authors had observed micro-cracks in the fusion zone which was reasoned to the segregation of S, Nb and Mo. Moreover the authors claimed that the EB weld process parameters required to be optimized for attaining proper welds.

It is evident from the literatures that electron beam welding is a successful technique to obtain dissimilar joints with good mechanical and metallurgical properties. In spite of the industrial applications demanding the need for joining Inconel 625 and UNS S32205, limited studies have been carried out on these bimetallic joints. The novelty of this study is the use of electron beam source for joining Nickel based superalloy and Duplex stainless steel. This study addressed in detail the structure – property relationships of EB weldments using the optical microscopy (OM) and scanning electron microscopy (SEM) techniques. Also the line mapping analysis was carried out across the weldments to understand the elemental movement during the process. The outcomes of this study will be highly beneficial to the industries demanding the need of these bimetals especially in geothermal and marine applications.

2. Experimental procedure

2.1. Base metals and welding procedure

The as-received base metals were cut to the dimensions of 20 × 20 × 5 mm to carry out chemical composition analysis using wet spectroscopic methods. The nominal chemical composition of the base and filler metals employed in the present investigation is represented in Table 1. The microstructure of the base metals Inconel 625 and UNS S32205 is shown in Figs. 1a and 1b. Further

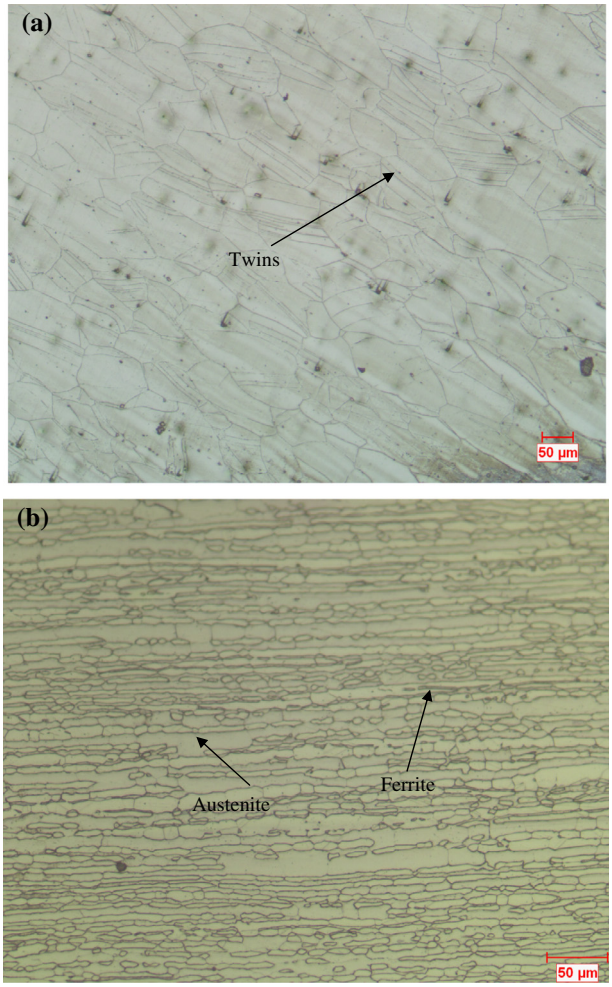

Fig. 1a. Microstructure showing the base metal of (a) Inconel 625 (b) UNS S32205.

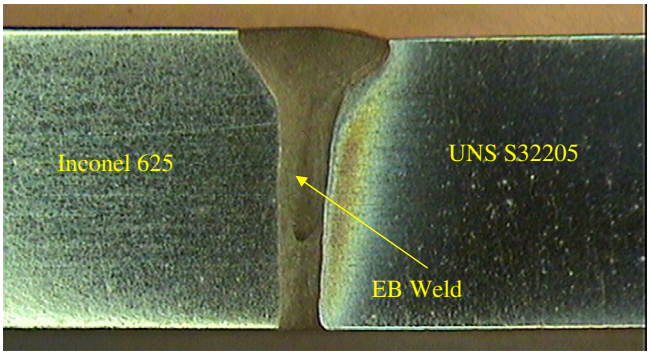

Fig. 1b. Cross-section macro-graph of EB welded Inconel 625 and UNS S32205.

the base metals of dimensions 170 mm × 50 mm × 5 mm were sliced using the Wire-cut Electrical Discharge Machining (WEDM) process to carry out welding.

Table 1
Chemical composition of the base/filler metals.

Base/filler metal	Composition (% Weight)								
	C	Mn	Cr	Mo	Fe	Nb	Ni	N	Others
Inconel 625	0.022	0.169	22.80	9.33	4.24	2.98	Rem.	–	Si – 0.104; Cu – 0.157; P – 0.004; S – 0.010; Al – 0.101; Co –<0.005; Ti – 0.235; Ta –<0.02
UNS S32205	0.028	1.32	23.16	3.19	Rem.	–	5.20	0.149	Si – 0.372; P – 0.026; S – 0.005

Table 2
Process parameters employed in EBW.

Process Parameters	Unit	Value
Accelerating voltage	kV	90
Beam current	mA	25
Beam focus	mA	1060
Travel speed	mm/min	1200
Heat input	kJ/mm	0.1125

The weld process parameters were established based on the iterative trials and the parameters chosen for the current study are shown in Table 2. Ensued to welding, the EB weldments were subjected to gamma ray Non-Destructive Testing (NDT) technique to determine for any surface/sub-surface defects. It was well observed from the study that the weldments obtained from the EB welding process was absolutely free from porosity, inclusions, cracks, under-cuts etc. Based on the NDT results, the welded specimens were further subjected to different metallurgical and mechanical characterization, and are outlined in the subsequent chapters.

2.2. Metallurgical and mechanical characterization of dissimilar weldments

The as-welded samples were cut to different coupons using WEDM process to investigate the metallurgical and mechanical properties. Microstructure examination and hardness measurement was carried out on the cross-sectioned coupons termed as "composite zone" (covering all the zones vis-à-vis parent metals and the weld zone of EB weldment) whose dimensions are 28 mm × 10 mm × 5 mm obtained by keeping the weld as center. Standard metallographic procedures including polishing with emery sheets of SiC with grit size varying from 220 to 1000 followed by disc polishing using alumina and distilled water were employed on these coupons to obtain a mirror finish of 1 μ on the weldments. Electrolytic etching (10% oxalic acid; 6 V DC supply; Current density 1.6 A/cm^2) was employed to reveal the grain structure of the different zones of the weldments. Micro-hardness studies were carried out on the coupons both in transverse and longitudinal direction to portray the variations across the weldment. Hardness measurements were carried out using Vicker's Micro-hardness tester employing a standard load of 500 gf for a dwell period of 10 s and at regular intervals of 0.25 mm. Transverse tensile studies were carried out on the coupons prepared as per the ASTM: E8/8M standards using Instron universal testing machine. The cross-head velocity was set to 2 mm/min to produce a strain rate of 3.3×10^{-4} s^{-1}. This strain rate is well in the range as prescribed by ASM International handbook of Mechanical Testing and Evaluation [12]. To study the response of the weldments to sudden loads, Charpy V-notch impact studies were also carried out on the sub-sized samples (55 mm × 10 mm × 5 mm) fabricated as per ASTM: E23-12c standards. Notches were made in such a way that the fracture occurred only within the weld fusion zones.

3. Results

3.1. Base metals

Microstructure studies showed that the base metal Inconel 625 contained the elongated, coarser austenitic grains with the presence of twin boundaries and some inter-metallic tiny, dark phases; whereas a dual phase microstructure was observed at UNS S32205 containing almost equal amounts of ferrite (54%) and austenite (46%) as inferred from the ferrite measurement study through Fischer Ferritoscope. The average tensile strength of the base metals was observed to be 915 MPa (Inconel 625) and 840 MPa (UNS S32205). Similarly the impact toughness was found to be 165 J for Inconel 625 and 220 J for UNS 32205.

3.2. Macro and microstructure examination

Cross-sectional macrograph of EB welds Inconel 625 and UNS S32205 is shown in Fig. 1b. It is evident that proper fusion with narrow bead was obtained on employing the EB welding technique. No visible cracks were observed during and after welding. The microstructures at the different zones are represented in Fig. 2a. It was well inferred from the interfacial microstructures shown in Fig. 2b that there were no significant grain changes observed at the regions adjacent to the fusion zone. Both the cellular and dendritic growth was observed at the fusion zone. Also the fusion zone adjacent to Inconel 625 side was observed to have fine, equiaxed grain growth. The interface microstructures were further investigated using SEM/EDAX analysis and are shown in Fig. 3. The fusion zone and the HAZ of Inconel 625 showed the presence of white, tiny phases which are enriched with Nb and Ti content. Similarly the fusion zone adjacent to UNS S32205 side was observed to have secondary phases with higher amounts of Mo.

Line mapping analysis was carried out at the interface of both the metals and the results are shown in Fig. 4. It was inferred that the elements Fe, Cr had been moved from the UNS S32205 to the

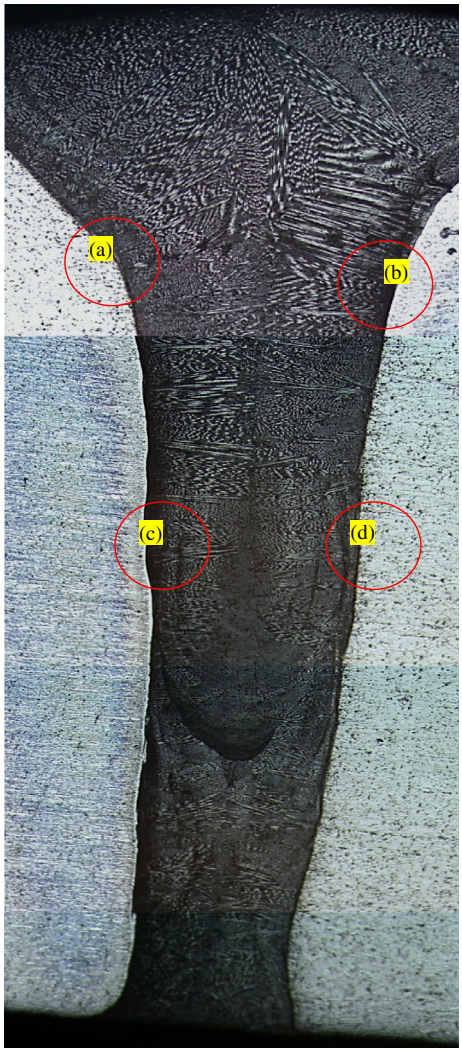

Fig. 2a. Microstructure of EB welded Inconel 625 and UNS S32205.

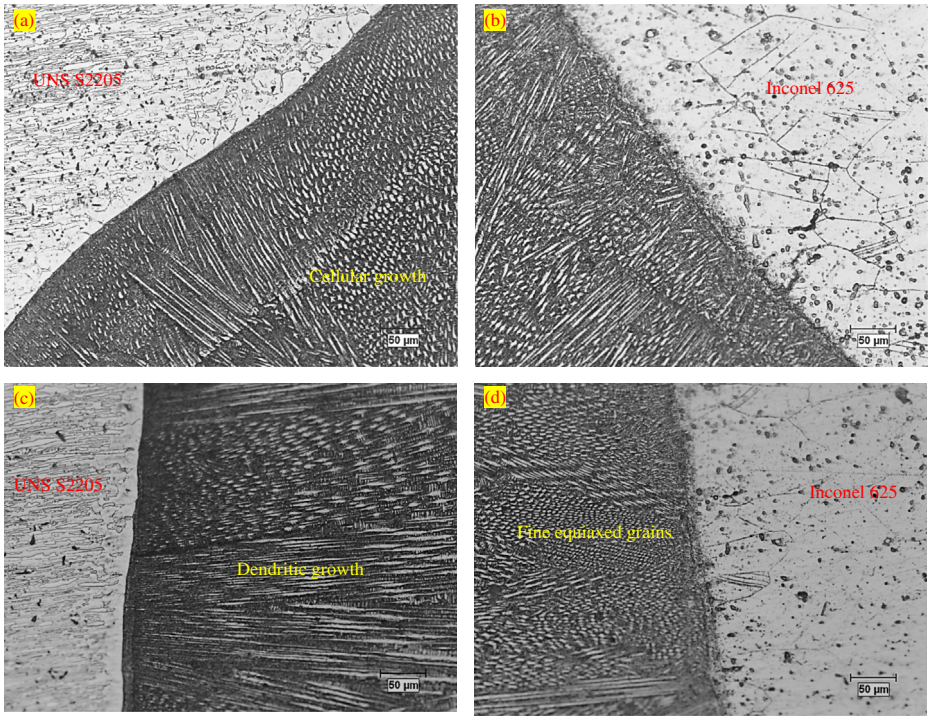

Fig. 2b. Microstructure showing the dissimilar welds of Inconel 625 and UNS S32205.

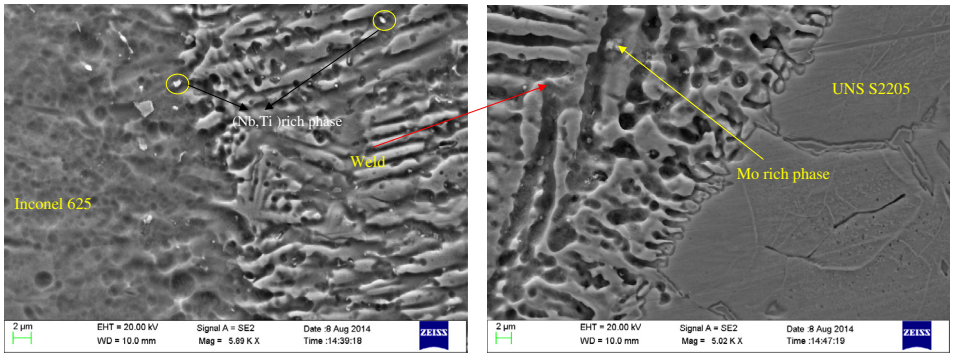

Fig. 3. Interface micrographs of the dissimilar weldments of Inconel 625 and UNS S32205 using SE Microscopy.

weld zone whereas the elements Ni, Nb and Mo were moved from Inconel 625 to the weld zone. Also the line mapping analysis across the weld zone was carried out and shown in Fig. 5b. SEM analysis showed the weld zone containing the dendrites and arms with the presence of secondary phases. The line mapping analysis showed that the dendritic body was observed to have fewer amount of Mo and the phases occupying the inter-dendritic arms containing Mo rich precipitates. It was further established by the point analysis shown in Fig. 5a.

3.3. Mechanical characterization

3.3.1. Hardness measurements

Hardness measurements were carried out in both longitudinal as well as in transverse direction of the weldment. The average hardness of the entire weldment in the longitudinal direction was observed to be 258 HV and, the average hardness value at the weld zone was observed as 240 HV. Similarly the average hardness values of 227, 225 and 218 HV were observed at the fusion zone adjacent to the Inconel 625, middle zone and the fusion zone adjacent to UNS S32205 respectively. The hardness plots both in transverse and longitudinal section of the weldment is shown in Fig. 6.

3.3.2. Tensile and impact studies

Tensile properties were ascertained to establish the response of the EB weldments to the gradually increasing load. The test results portrayed that the weldments undergo failure at the weld zone in all the trials [Fig. 7a] and the average tensile strength and 0.2% proof strength were reported to be 850 and 345.5 MPa [Table 3]. SEM morphology of the fractured EB welds revealed the presence of micro-voids running in the fibrous, shiny tearing ridges [Fig. 7b]. Further Charpy V-notch impact studies were carried out on the coupons prepared as per the ASTM E23-12C standards. It was observed from the impact tests [Fig. 8a] that the EB welds had undergone severe rupture and were broken into two equal halves. The average impact toughness of the EB weldments was established to be 26 J. SEM fractograph of the impact tested sample showed the scarce voids with the cleavage facets appearing to have beach sand ridges [Fig. 8b]. Also the presence of secondary phases

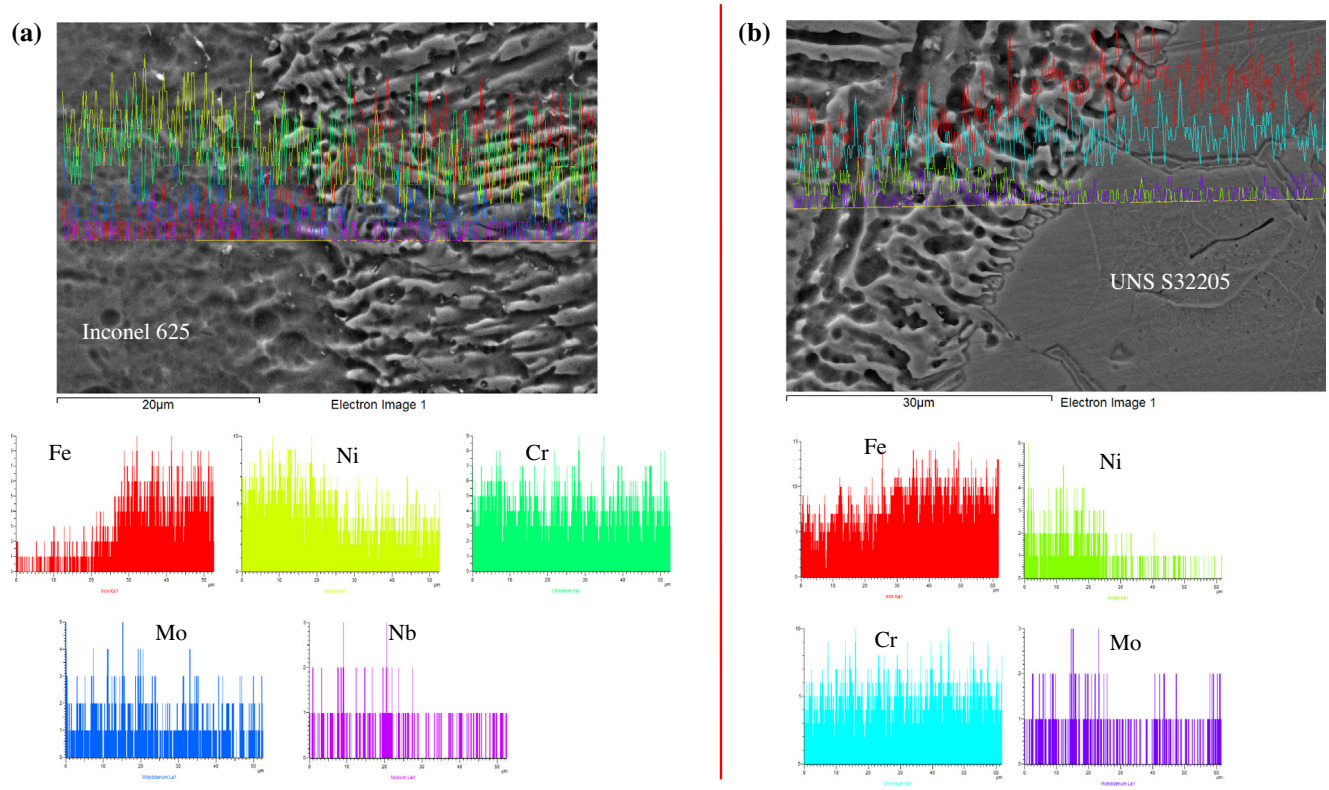

Fig. 4. Line mapping analysis along the weld interface of (a) UNS S32205 and (b) Inconel 625.

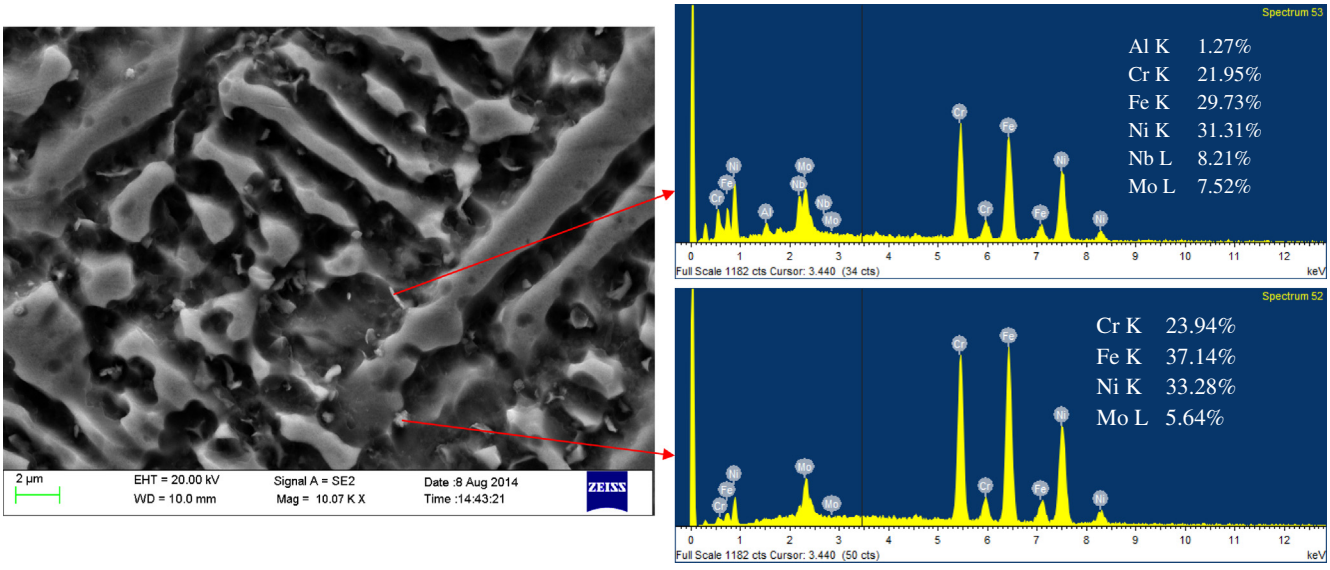

Fig. 5a. SEM/EDAX point analysis on the weld zone of the EB welded Inconel 625 and UNS S32205.

was observed at the void spaces and also in the cracked boundaries.

4. Discussion

Macrostructure studies inferred that the narrow bead with complete fusion of Inconel 625 and UNS S32205 could be achieved successfully by EB welding technique. Microstructure studies also clearly conveyed the absence of grain coarsening effects at the HAZ of UNS S32205 and Inconel 625. This could be reasoned to the controlled, lower high heat inputs and faster cooling rates developed during EBW process. Fine equiaxed cellular and dendritic grain growth was observed at the fusion zone. The middle of the fusion zone showed fine, uniform equiaxed cellular structure which shall be attributed to more uniform and symmetric cooling compared to the sides or edges of the fusion zone. Moreover the columnar dendritic formation shall be due to the lower thermal conductivity of Inconel 625 (9.8 W/m°C at 20 °C) in comparison to UNS S32205 (14 W/m°C at 20 °C) which resulted in small heat dissipation in this area. Similarly no solidification cracking was observed at the fusion as well as in the adjacent zones which

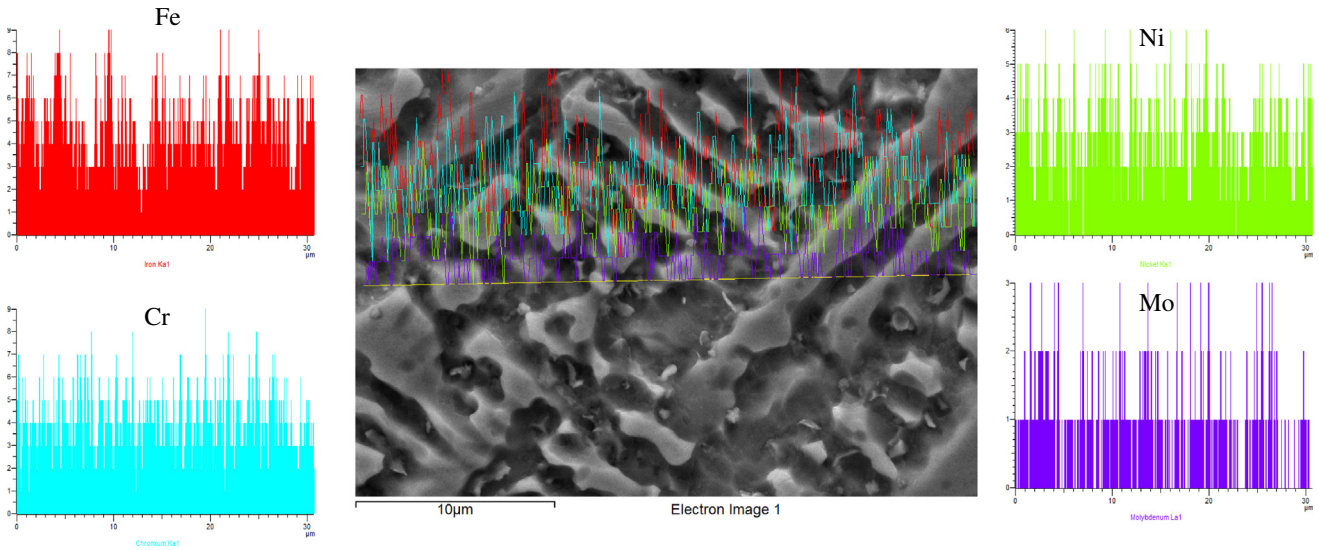

Fig. 5b. Line mapping analysis on the weld zone of EB welded Inconel 625 and UNS S32205.

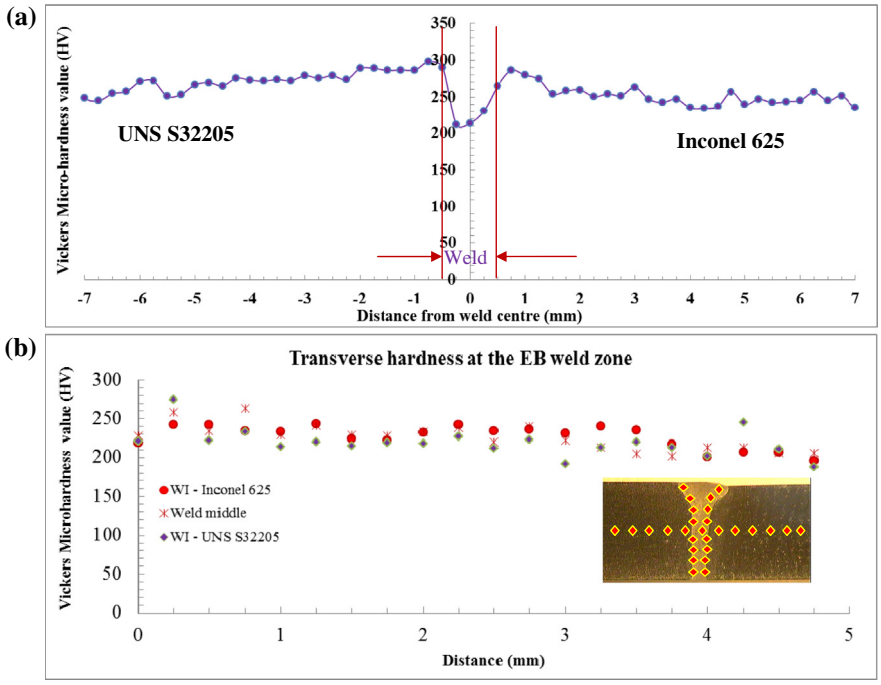

Fig. 6. Hardness profile of EB weldments (a) longitudinal and (b) transverse section of the weld.

clearly indicated that the process parameters employed in the study were optimal. Ferrite measurements were carried out at different locations of EB weldments using Fischer Ferritoscope. It was inferred that the bottom and top of the weld zone contained 10.5% and 4.9% respectively. Also these results clearly portrayed that the solidification mode was either completely austenitic (A) or austenitic – ferritic (AF).

Line mapping analysis was carried out to infer the elemental movement during the welding process. The elements Ni, Nb and Mo from Inconel 625 side and Fe, Cr from the UNS S32205 were migrated to the weld zone. It is well understood from Fig. 4(a) and (b) that the fusion zone obtained from the EBW process resulted in enrichment of the aforementioned elements. The results of line mapping analysis on the fusion zone shown in Fig. 5b observed to have the presence of Ni, Fe at the dendritic and inter-dendritic regions; whereas the element Mo was found to be greater at the inter-dendritic zones compared to dendritic cores. It is also well supported by the SEM/EDAX point analysis which indicated the presence of Mo, Nb rich phases segregated at the dendritic arms appeared as tiny, white splats [Fig. 5a]. This could be explained as Mo and Nb have large radii in comparison to the other elements in the molten pool, causing segregation during the terminal solidification. It was evident from Fig. 3 the formation of Nb, Ti rich phases which appeared as tiny splats at the fusion and HAZ zone of Inconel 625.

Hardness measurements showed the weld hardness was slightly plummeted compared to the base metals. The hardness measurements at the transverse sections indicated that the

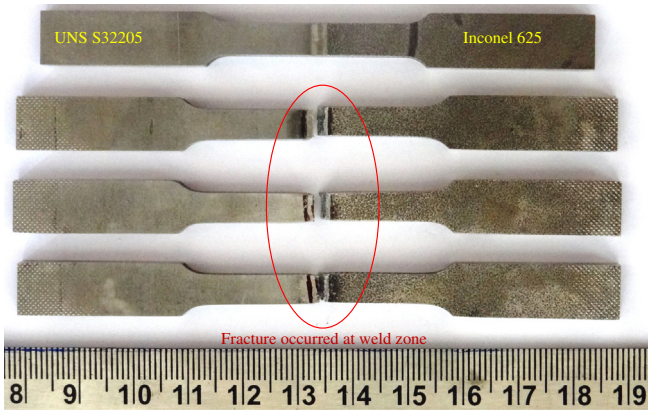

Fig. 7a. Tensile studies on the EB weldments of Inconel 625 and UNS S32205 showing the fracture at the weld zone in the trials.

Table 3
Tensile properties of the dissimilar weldments of Inconel 625 and UNS S32205.

Property	Unit	Trial 1	Trial 2	Trial 3	Average
Maximum load	kN	26.03	26.21	26.01	**26.095**
Ultimate tensile strength	MPa	850.0	851.0	849.0	**850.0**
0.2% Proof strength	MPa	345.71	343.26	347.37	**345.45**
Ductility	%	20.43	24.24	23.97	**22.88**
Fracture zone	–	Weld zone			

average hardness at the fusion zone adjacent to Inconel, middle of the weld and fusion zone adjacent to UNS S32205 were observed to be 227, 225 and 218 HV respectively which is slightly lower as compared to the parent metals. The lower hardness values at the fusion zone shall be reasoned to the presence of tensile residual stresses developed during EBW process and also this might be due to the differences in chemical composition and coefficients of thermal expansion of the base metals. As reported by Joseph et al. [13], if the energy input to welding speed ratio increases the hardness value of the weld zone would decrease. Moreover solid solution strengthening elements such as Mo and Nb could not dissolve completely during solidification and caused

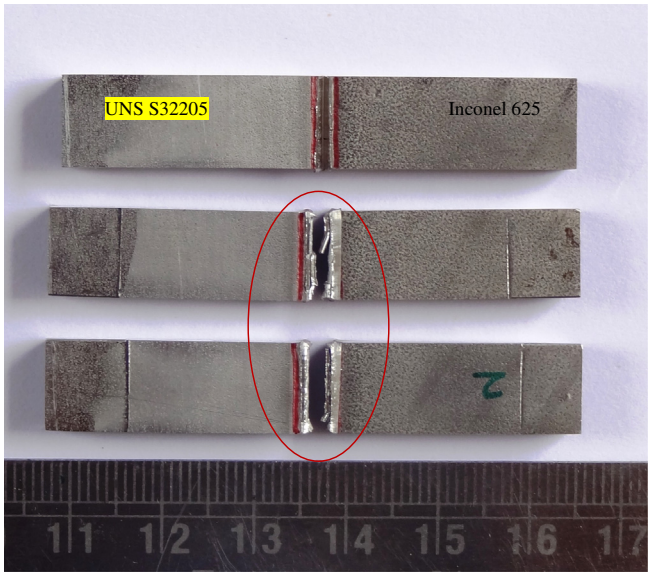

Fig. 8a. Impact tested EB weldments of Inconel 625 and UNS S32205 observing the fracture at the weld zone.

segregation which also augmented for the same. The hardness at the weld interface of Inconel 625 was found to be 286 HV, which may be reasoned to the formation of enriched amount of Nb, Ti rich phases and is well observed from the microstructure studies.

Similarly the tensile studies showed that in all the trials, the failure occurred at the fusion zone. The average ultimate tensile strength and proof strength of the EB welds were reported to be 850 MPa and 345.5 MPa with the average ductility of 22.9%. It is inferred from the tensile studies that the weld strength was found to be greater than one of the parent metals, UNS S32205 (840 MPa). Hence it is proven that the EB welds of Inconel 625 and UNS S32205 resulted in joints with higher or almost same strength as base metal. This outcome has been considered to be the major breakthrough from the study. The tensile results of EB welds were greater compared to the earlier works of the authors who reported the GTA weldments of Inconel 625 and Duplex

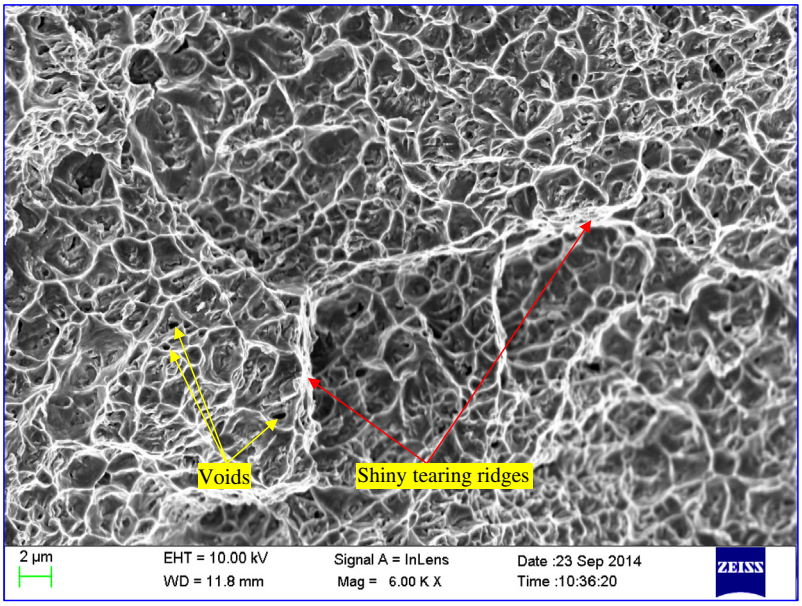

Fig. 7b. SEM fractograph of the tensile tested EB weldments of Inconel 625 and UNS S32205.

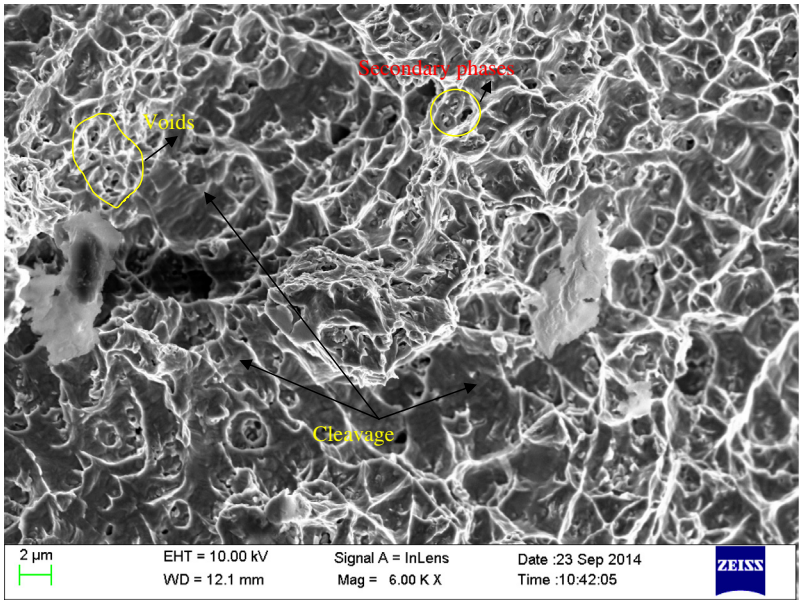

Fig. 8b. SEM fractograph of the impact tested EB welds.

stainless steel [4]. The fine, equiaxed grains observed in the fusion zone facilitated favorably for more dislocations and pinning actions during the tensile loading which probably improved the strength of the EB weldments. Also the ferrite measurement results nurtured the presence of minimum and maximum amounts of ferrite in the EB fusion zone improved the weld strength. The presence of ferrite refines the grain size of the solidified metal, which results in better mechanical properties and cracking resistance [14]. However, the reason for fracture occurring at the EB weld zone could be well attributed to the segregation of Mo rich phases at the inter-dendritic zones. It could be understood from the ferrite measurement studies that the EBW resulted in higher amounts of austenite. As reported by Perricone and Dupont [15], the austenite grains did not readily diffuse Mo and resulted in segregation. The authors further reported the solubility of Mo was lesser in the Fe based alloys.

It was inferred from the impact test results that the EB welds resulted in toughness value of 26 J which was much lower as compared to the base metals. SEM fractograph of the impact tested weldment corroborated the presence of scarce voids and cleavage facets dominated in the fractured surface which clearly inferred that the mode of fracture was brittle in nature. Also the visual examination showed that the weldments were broken into two halves upon impact loading. As noticed from the SEM/EDAX analysis, the Mo rich phases were segregated at the inter-dendritic regions and would be reasoned for low energy absorption. This could be well reflected in the SEM fractograph in terms of the secondary phases nucleated from the voids and in the cracked grain boundaries. Several researchers [6,16,17] investigated the EB welding of duplex/super-duplex stainless steel which resulted in the formation unbalanced ferrite – austenite ratio in the weld zone and contributed for lower impact toughness. Draugelates et al. [18] reported that higher cooling rates suppress the diffusion-controlled processes in austenite reformation. Low heat input would normally result in undesirable proportion of ferrite in weld and in corresponding loss of toughness [19]. As reported by Muthupandi et al. [16], the Cr_2N precipitation could be favored during EB welding due to faster cooling rates. Even though it was not explicitly observed in the SEM/EDAX analysis, TEM analysis is required to confirm the presence of this phase which was not reported in the present study. Segregation was noticed at the fusion zone which may also cause a decrease in impact toughness values. Similar observations were reported by Yılmaz and Tümer [20]. As reported by Khodir et al. [21], reduction in toughness values was observed in high strength 3–9% Ni-steel alloys metals when the nickel content was gradually increased from 3% to 5%. In the present study, the SEM/EDAX analysis showed the higher amounts of Ni in the EB fusion zone which also impoverished the toughness.

In a nutshell, this study articulated the EBW of dissimilar metals involving Inconel 625 and UNS S32205 for the first time. The results portrayed the absence of grain coarsening effects and other metallurgical problems at the regions adjacent to the fusion zone. Tensile studies reported the weld strength of EB weldment was greater compared to other GTA welding process [4]. However the impact toughness of EB weldments was impoverished which needs further investigations by varying the process parameters or doing post weld heat treatments.

5. Conclusions

This study reported the dissimilar welds of Inconel 625 and UNS S32205 obtained by EB welding process and the following conclusions are deduced.

(1) Successful, defect free joints of Inconel 625 and UNS S32205 duplex stainless steel could be obtained by Electron beam welding process.
(2) There was no significant grain coarsening or other negative metallurgical effects observed at the heat affected zones. The formation of fine, cellular dendritic structure at the EB fusion zone was due to the controlled low heat input and higher cooling rates developed during the process.
(3) Tensile studies corroborated the failures occurred at the weld zone which was predominantly due to the segregation of Mo rich phases. However the weld tensile strength was greater than or equal to the strength of UNS S32205.
(4) Impact toughness of the EB weldments was impoverished due to the presence of secondary phases at the fusion zone.

Acknowledgement

The authors are grateful to acknowledge the Department of Science and Technology (DST) for providing the UTM facility to our VIT University under DST-FIST.

References

[1] van Wijngaarden Michael, Chater James. CalEnergy goes for duplex. Stainless Steel World; 2006. 42.
[2] Richard OB. Subsea structure demands high-quality GTA pipe welds. <http://www.aws.org/wj/june02/feature2.html>; [dated 29.09.14].
[3] Vandervoort RR. Mechanical properties of Inconel 625 welds in 21-6-9 stainless steel at 4 K. Cryogenics 1979;19(8):448–52.
[4] Sridhar R, Devendranath Ramkumar K, Arivazhagan N. Characterization of microstructure, strength, and toughness of dissimilar weldments of Inconel 625 and duplex stainless steel SAF 2205. Acta Metall Sinica (English Lett) 2014. http://dx.doi.org/10.1007/s40195-014-0116-5.
[5] Sindo Kou. Welding metallurgy. 2nd ed. Hoboken, New Jersey: John Wiley & Sons Inc.; 2003.
[6] Devendranath RK, Debidutta M, Vignesh MK, Ganesh RB, Arivazhagan N, Shah VN, Suresh Kumar S. Metallurgical and mechanical characterization of electron beam welded super-duplex stainless steel UNS 32750. J Manufact Process 2014;16:527–34.
[7] Sun Z, Karppi R. The application of electron beam welding for the joining of dissimilar metals: an overview. J Mater Process Technol 1996;59:257–67.
[8] Patterson RA, Milewski JO. GTA weld cracking-alloy 625 to 304L. Weld J 1985;64(8):227–231s.
[9] Madhusudan Reddy G, Srinivasa Rao K. Microstructure and mechanical properties of similar and dissimilar stainless steel electron beam and friction welds. Intl. J Adv Manuf Technol 2009;45:875–88.
[10] Venkata Ramana P, Madhusudhan Reddy G, Mohandas T, Gupta AVSSKS. Microstructure and residual stress distribution of similar and dissimilar electron beam welds – maraging steel to medium alloy medium carbon steel. Mater Des 2010;31:749–60.
[11] Shakil M, Ahmad M, Tariq NH, Hasan BA, Akhter JI, Ahmed E, et al. Microstructure and hardness studies of electron beam welded Inconel 625 and stainless steel 304L. Vacuum 2014. http://dx.doi.org/10.1016/j.vacuum.2014.08.016.
[12] ASM handbook on mechanical testing and evaluation. ASM International, vol. 8; 2000.
[13] Joseph Benjamin, Katherasan D, Sathiya P, Srinivasa Murthy CV. Weld metal characterization of 316L(N) austenitic stainless steel by electron beam welding process. Int J Eng, Sci Technol 2012;4(2):169–76.
[14] Shankar V, Gill TPS, Mannan SL, Sundaresan S. Solidification cracking in austenitic stainless steel welds. Sadhana 2003;28(3 & 4):359–82.
[15] Perricone MJ, Dupont JN. Effect of composition on the solidification behavior of several Ni–Cr–Mo and Fe–Ni–Cr–Mo Alloys. Metall Mater Trans A 2006;37A:1267–80.
[16] Muthupandi V, Bala Srinivasan P, Seshadri SK, Sundaresan S. Effect of weld metal chemistry and heat input on the structure and properties of duplex stainless steel welds. Mater Sci Eng, A 2003;358:9–16.
[17] Jang Seok-Hwan, Kim Soon-Tae, Lee In-Sung, Park Yong-Soo. Effect of shielding gas composition on phase transformation and mechanism of pitting corrosion of hyper duplex stainless steel welds. Mater Trans 2011;52(6):1228–36.
[18] Draugelates U, Schram A, Boppert C, Liu J. Proc duplex stainless steel'91 1991;2:977–84.
[19] Schwarz L, Vrtochová T. Study of solidification and structural modifications of duplex and superduplex steels. Welder 2010;7(1):7–10.
[20] Yılmaz Ramazan, Tümer Mustafa. Microstructural studies and impact toughness of dissimilar weldments between AISI 316 L and AH36 steels by FCAW. Int J Adv Manuf Technol 2013;67:1433–47.
[21] Khodir S, Shibayanagi T, Takahashi M, Abdel-Aleem H, Ikeuchi K. Microstructural evolution and mechanical properties of high strength 3–9% Ni-steel alloys weld metals produced by electron beam welding. Mater Des 2014;60:391–400.